ELSEVIER

Biophysical Chemistry 111 (2004) 213–222

Biophysical Chemistry

www.elsevier.com/locate/bpc

Characteristics of structure, composition, mass spectra, and iron release from the ferritin of shark liver (*Sphyrna zygaena*)

He-Qing Huang[a,b,*], Zhi-Qun Xiao[a], Xu Chen[a], Qing-Mei Lin[b,c], Zong-Wei Cai[d], Ping Chen[a]

[a] *Department of Biology, School of Life Sciences, The Key Laboratory for Chemical Biology of Fujian Province, Xiamen University 361005, China*
[b] *The Key Laboratory of Marine Environmental Science (Ministry of Education), Xiamen University, Xiamen 361005, China*
[c] *The Key Laboratory of MOE for Cell Biology and Tumor Cell Engineering, Xiamen University, Xiamen 361005, China*
[d] *Department of Chemistry, Hong Kong Baptist University, Kowloon Tong, Hong Kong*

Received 10 April 2004; received in revised form 4 June 2004; accepted 4 June 2004
Available online 2 July 2004

Abstract

The ferritin consists of a protein shell constructed of 24 subunits and an iron core. The liver ferritin of *Sphyrna zygaena* (SZLF) purified by column chromatography is a protein composed of eight ferritins containing varying iron numbers ranging from 400 ± 20 Fe^{3+}/SZLF to 1890 ± 20 Fe^{3+}/SZLF within the protein shell. Nature SZLF ($SZLF_N$) consisting of holoSZLF and SZLF with unsaturated iron ($SZLF_{UI}$) to have been purified with polyacrylamide gel electrophoresis (PAGE) exhibited five ferritin bands with different *p*I values ranging from 4.0 to 7.0 in the gel slab of isoelectric focusing (IEF). HoloSZLF purified by PAGE ($SZLF_E$) not only had 1890 ± 20 Fe^{3+}/$SZLF_E$ but also showed an identical size of iron core observed by transmission electron microscopy (TEM). Molecular weight of ~ 21 kDa for $SZLF_E$ subunit was determined by sodium dodecyl sulfate-polyacrylamide gel electrophoresis (SDS-PAGE). Four peaks of molecular ions at mass/charge (*m*/*z*) ratios of 10611.07, 21066.52, 41993.16, and 63555.64 that come from the $SZLF_E$ were determined by matrix-assisted laser desorption ionization/time-of-flight mass spectrometry (MALDI-TOF MS), which were identified as molecular ions of the ferritin subunit (M^+) and its polymers, namely, $[M]^{2+}$, $[M]^+$, $[2M]^+$, and $[3M]^+$, respectively. Both $SZLF_E$ and a crude extract from shark liver of *S. zygaena* showed similar kinetic characteristics of complete iron release with biphasic behavior. In addition, a combined technique of visible spectrometry and column chromatography was used for studying ratio of phosphate to Fe^{3+} within the $SZLF_E$ core. Interestingly, this ratio maintained invariable even after the iron release, which differed from that of other mammal ferritins.

Keywords: Liver ferritin; Shark; MALDI-TOF MS; Kinetics of iron release; Composition; Tumor

1. Introduction

Ferritins are ubiquitous proteins found in bacteria, plants, and animals where they play important roles in maintaining iron level in a soluble, nontoxic bioavailable form [1–5]. Ferritins are composed of 24 subunits arranged to form a protein shell of 120 Å in diameter enclosing a central cavity of 70–80 Å diameter for iron storage [6,7]. Very little information of mass spectra from the ferritins has been reported by various techniques of mass spectrometry such as matrix-assisted laser desorption/ionization time of flight mass spectrometry (MALDI-TOF MS) and electrospray ionization (ESI)-TOF MS.

The kinetic study of iron release is a valid method for elucidating the process of iron entry and exit and for analyzing stability of the ferritin core [3,8,9]. Most experimental results show that the kinetic curves of complete iron

Abbreviations: SZLF, liver ferritin of *Sphyrna zygaena*; HSF, horse spleen ferritin; AvBF, bacterial ferritin of *Azotobacter vinelandii*; IEF, isoelectric focusing; HLF, human liver ferritin; PSFF, pig spleen ferritin-Fe; PSF, pig spleen ferritin; PAGE, polyacrylamide gel electrophoresis; $SZLF_{UI}$, SZLF consisted of unsaturated iron within the protein shell; $SZLF_N$, nature SZLF consisted of holoSZLF and $SZLF_{UI}$; $SZLF_{55\%}$, 55% ($SZLF_{UI}$) of total $SZLF_N$; $SZLF_{45\%}$, 45% (holoSZLF) of total $SZLF_N$; $SZLF_{45\%E}$, $SZLF_{45\%}$ purified by PAGE; $SZLF_E$, holoSZLF purified by PAGE; $SZLF_{EU}$, $SZLF_E$ with unsaturated iron because of iron release; $DALF_E$, holoDALF purified by PAGE; HSF_E, holoHSF purified by PAGE; TFA, trifluoroacetic acid; SF, serum ferritin; TF, tissue ferritin; SA, sinapic acid; DHB, 2,5dihydroxybenzoic acid; TEM, transmission electron microscope; P_i, inorganic phosphate; SDS-CGE, sodium dodecyl sulfatecapillary gel electrophoresis; SDS-PAGE, sodium dodecyl sulfate-polyacrylamide gel electrophoresis; MALDI-TOF MS, matrix-assisted laser desorption/ionization time of flight mass spectrometry; ESI, electrospray ionization.

* Corresponding author. Department of Biology, School of Life Sciences, The Key Laboratory for Chemical Biology of Fujian Province, Xiamen University, Xiamen 361005, China. Tel.: +86-592-2186392; fax: +86-592-2186630.

E-mail address: hqhuang@xmu.edu.cn (H.-Q. Huang).

0301-4622/$ - see front matter © 2004 Elsevier B.V. All rights reserved.
doi:10.1016/j.bpc.2004.06.002

release does not follow laws of zero-, first-, or second-order reactions [10–13]. A biphasic behavior of complete iron release from the mammal and bacterial ferritins has been employed to explain for this complex kinetic process [11,13]. Both authors indicated that ferritins simultaneously released the iron as first-order reaction on the surface of the protein core and as zero-(or first-)order reaction on the inside of the core. However, the formation reasons of the variable orders and biphasic behavior for complete iron release from the ferritins coming from different species are still unclear and disputable.

The core compositions, consisted of iron and inorganic phosphate from the mammal and bacterial ferritins, have given different results [5,6,14]. It is summarized that the average ratios of total phosphate to iron within the protein core are 1:131 for pig spleen ferritin-Fe (PSFF), 1:13 for pig spleen ferritin (PSF), 1:9 for horse spleen ferritin (HSF), and 1:1.2 for *Azotobacter vinelandii* of bacterial ferritin (AvBF), respectively [9,15]. The ratio varies along with increment of the iron release. Interestingly, the iron structure with a 1:3 ratio of phosphate to iron was found on the surface of HSF core by various pH ranging from 5.0 to 10.0 [1,14], which ratio is higher than the average that of the whole HSF core. Moreover, Johnson et al. [16] reported that an inorganic phosphate (P_i) layer consisted of Fe^{2+} and P_i at a 1:3 ratio was strongly attached to the reconstituted ferritin core surface and was stable even after air oxidation of the bound Fe^{2+}. Thus, it was concluded that different average ratio from the ferritin cores resulted from different species. Its role, however, remains questionable in understanding the ferritin behavior of iron release and storage.

Typically, most ferritins in nature are composed of 24 subunits of H and L chains, which are functionally distinct. The ferritin containing high levels of iron in living cells tend to be rich in L chains and may have a long-term storage function, whereas H-rich ferritins are more active in iron metabolism [17]. Many analytical techniques, such as sedimentation velocity, normal electrophoresis, and capillary gel electrophoresis, have been developed to study the type of subunits and to measure its H/L ratio among the ferritins [18–22]. Human ferritin can be classified into serum ferritin (SF) and tissue ferritin (TF), which consists of subunits with two types, light (L) chain (19.0 kDa) and heavy (H) chain (21.0 kDa). Like SF and TF, other mammal ferritins consist of two subunits of H- and L-types [3,23,24], which suggests that H-subunit contains a ferroxidase site oxidizing Fe^{2+} to Fe^{3+} and that L-subunit has a cluster of acidic residues that are believed to be involved in the core formation. Furthermore, the electrophoresis studies reveal that the ferritins isolated from the bullfrog tadpole blood consist of three subunit types (H-, M-, and L-subunits), and from the bacteria consist of single subunit type only [25]. In addition, the ferritins isolated from different fish livers of equine, murrel, rohu, mackerel, salmon, and perch are composed of single subunit type of 21 kDa rather than two subunit types in the SDS-gel, indicating the presence of similar-sized subunits in the native fish ferritins [26]. Moreover, *Escherichia coli* with recombinant gene of human ferritin is able to express two ferritins, which are a human ferritin consisted of H and L subunit types and a bacterial ferritin consisted of single subunit type at the same time [23,27] because of the gene expression. Even so, the real roles of the subunits including the types coming from the different species for iron release and storage are still unclear.

Research of recent years shows that level of serum ferritin as a marker has widely been used to diagnose whether human or other animals have caught the tumors [28,29]. Though the shark is also a vertebrate, the diagnose cases of various cancers from shark have not been reported in details. In addition, the tumor diseases have not been found in the bacteria having the ferritins consisted of single subunit type, but it has widely been found in mammals having the ferritins consisted of two subunits (H and L). It is for the reason that we want to know whether the molecular structure of liver ferritin of *Sphyrna zygaena* (SZLF) consists, like bacterial ferritin, of single subunit type and the interaction force among SZLF subunits weaken.

In this paper, we present several analytical methods such as transmission electron microscope (TEM) and column chromatography, MALDI-TOF MS and electrophoresis for measuring the molecular structure, the characteristics of mass spectra, the chemical composition of the iron core, and the kinetics of iron release from the $SZLF_E$. These techniques have proven to be a useful tool in explaining the mechanism of iron storage and release in vivo and many unclear questions in the ferritin research.

2. Materials and methods

2.1. Materials

Fresh shark, *S. zygaena*, was purchased from Xiamen Fish, Xiamen, China. DEAE-cellulose 52 was obtained from Waterman (Breman, Germany). Sephadex G-25 and Sephacryl S-300 HR are products of Pharmacia (Uppsala, Sweden). Sinapic acid (SA), 2,5-dihydroxybenzoic acid (DBH) and all electrophoresis reagents were obtained from Sigma (Cleanse, USA). Other inorganic chemicals were analytical grade reagents obtained from commercial sources in China.

2.2. Methods

2.2.1. SZLF preparation and purification

A 1:2 weight ratio of shark liver to distilled water at pH 7.25 was mixed after removal of the lymph and fat tissue. The mixed sample was homogenized at 8000 rpm. The homogenate was heated to 75–80 °C in a water thermostat for 5–7 min to denature most proteins except for SZLF. Next, the solution was filtered twice with 10 layers of gauze. A red-brown filtrate was collected after it was cooled. The

filtrate was centrifuged twice at $6 \times 1000 \times g$ for 60 min. The supernatant was collected.

The SZLF samples were further separated and purified by a column chromatography with a procedure described recently [30]. The collected ferritin is considered as $SZLF_N$ containing various iron numbers within the protein core. Although $SZLF_N$ has a different ratio of iron to phosphate within its core, it showed a single peak with high-performance liquid chromatography (HPLC) or a single band with polyacrylamide gel electrophoresis (PAGE).

2.2.2. Element and protein concentration analysis

Total Fe^{3+} levels in the ferritins were determined by an atomic absorbance spectrophotometer (PE-800 AA) after the proteins were nitrated. Phosphate content within the ferritin core was measured by a method described previously [31]. Measurement of the protein concentration was carried out by normal Lowry procedure. Bovine serum albumin of 99.0% purity was utilized as a protein standard.

2.2.3. Measurement of the ratio of phosphate to iron within the $SZLF_E$ core

First, solutions of 6.0 ml SZLF with saturated irons purified by PAGE ($SZLF_E$) at pH 7.25, 20 μl of α′ α-dipyridyl and 30 μl of dithionite were quickly mixed for 60 min under anaerobic condition for iron release. Next, the $SZLF_E$ with unsaturated iron ($SZLF_{EU}$) was separated on a Sephadex G-25 column (2×6 cm) that was preequilibrated with 0.025 M Tris–HCl (pH 7.25)/0.05 M NaCl for removing the released phosphate and iron and collecting the $SZLF_{EU}$ samples that would be used for the next reaction of iron release. The content of phosphate and iron within the $SZLF_{EU}$ core was determined by using the method of Cooper [31] and the atomic absorbance spectrophotometry, respectively, which are used to calculate the average ratio of phosphate to iron within the $SZLF_{EU}$ core. The reaction of iron release for the ratio calculation was done until 95% of total iron and phosphate within the $SZLF_{EU}$ core was completely removed.

2.2.4. Electrophoresis of $SZLF_E$

Three percent stacking and 5–14% gradient of acrylamide gels was performed for PAGE analysis of $SZLF_E$. The gel was run in a Tris (0.025 M, pH 8.3)–glycine (0.2 M) buffer at 80 V for 60 min and then at 150 V for 4 h. Isoelectric focusing (IEF) of $SZLF_E$ was performed in 4% gel with ampholines at pH ranging from 3.0 to 8.0. Before protein was stained, a segmental gel (1×0.5 cm) was excised along cathode to anode, immersed in doubly distilled water and stirred for 1.5 h. A pH meter equipped with a fine pH electrode was used to determine the pH gradient of the IEF gel.

2.2.5. $SZLF_E$ subunit preparation

The $SZLF_E$ was extracted and collected from the PAGE gel after it was scanned. The $SZLF_E$ subunit was separated by SDS-PAGE method as normally described, and its molecular weight was calculated according to a group of the markers of protein subunits (Sigma).

2.2.6. Electron microscopy of the ferritin

The $SZLF_E$ was prepared for the measurement of transmission electron microscopy (TEM) by air drying small drops of the solution. A drop of $SZLF_E$ was mounted onto the copper grids (400 mesh). Then, excess $SZLF_E$ was removed by cleaning the edge of the grid with a piece of filter paper. After the $SZLF_E$ was dried by air, a drop of phophotungstic acid (2%) was applied on the grids after being stained for 10 min, and the excess phophotungstic acid was removed with filter paper to allow the grid to be dried rapidly. The $SZLF_E$ was viewed and photographed on a JEM-100CXII Electron Microscope (JEOL, Japan) operating at 100 keV at 150,000 × magnifications. The measurement of 50 cores from enlarged photomicrographs was applied to determine the particle size of the ferritin.

2.2.7. Kinetics of iron release

A kinetic reaction in vitro for iron release from the $SZLF_E$ was carried out. Two and one-half milliliters of $SZLF_E$ (pH 7.25), 100 μl α′ α-dipyridyl, and 200 μl saturated dithionite were quickly mixed in an anaerobic cuvette filled with 99% Ar gas. Kinetics of complete iron release was determined by UV-240 Model spectrophotometer (Simadzu, Japan) at 520 nm. The data of iron release were recorded according to the desired time.

A 1:2 weight ratio of shark liver (2 g) to distilled water (4.0 ml) at pH 7.25 was mixed after removal of the lymph and fat tissue, and the mixture sample was homogenized at 8000 rpm. The homogenate solution was heated at 30 and 60 °C for 30 min, respectively, and then centrifuged at $10 \times 1000 \times g$ for 20 min. The supernatant (crude extraction) was collected, and then the sediment was discarded. Free Fe^{2+}/ Fe^{3+} and other metal ions in the extraction were removed by a method of membrane dialysis. The research model with purified extraction is considered as a kinetic process of complete iron release in vivo because of the presence of abundant various proteins and other biological molecules in the crude extraction.

2.2.8. MALDI-TOF-MS analyses

All MALDI-TOF-MS analyses were conducted by using a Bruker Reflex III (Berman, Germany) equipped with a 337 nm UV nitrogen laser producing 3 ns pulses. The mass spectra of ferritin and its subunit were obtained in the reflective mode. Mass assignments were performed with unmanipulated spectra for an optimal correlation between observed and calculated mass. Samples were prepared by the mixed solution containing acetone (10 μl) with a saturated solution of the matrix SA [in acetone containing 2% trifluoroacetic acid (TFA), 10 μl]. A portion (5 μl) of the mixed solution-containing matrix was loaded onto the target, and the solvent was removed by air

drying. Finally, the target-having sample was transferred to the mass spectrometer with optimal laser intensity for analysis.

3. Results and discussions

3.1. Various iron numbers within the $SZLF_N$ core

Liver ferritin from the shark (*S. zygaena*, SZLF) was purified by thermal denaturation and ammonium sulfate fraction, and further purified by gel exclusion chromatography. Chemical analysis of the SZLF by atomic absorbance spectrometry for iron measurement and by a Lowry method for protein analysis showed an average data with 1350 ± 100 Fe^{3+}/SZLF, indicating that the iron content from the SZLF were only half of that of HSF (2600 Fe^{3+}/HSF) reported recently [14]. In order to understand whether the iron numbers within the protein shell is an important factor to form complex kinetics of iron release with biphasic behavior, the SZLF sample is ulteriorly separated by a DEAE-52 column with gradient elution of NaCl ranging from 0.05 to 0.25 M (Fig. 1, right coordinate). The results of different absorbance peaks in Fig. 1(a–h) clearly showed that eight ferritin samples were collected by the various NaCl concentrations. Chemical analysis further showed that these proteins with variable iron numbers within its core (Fig. 1, left coordinate) are observed, which means that the native SZLF sample consists of holoSZLF and other SZLFs with unsaturated iron ($SZLF_{UI}$), which is called $SZLF_N$. It is indicated that $SZLF_{UI}$ plays an important role in storing the surplus iron for iron metabolism in vivo.

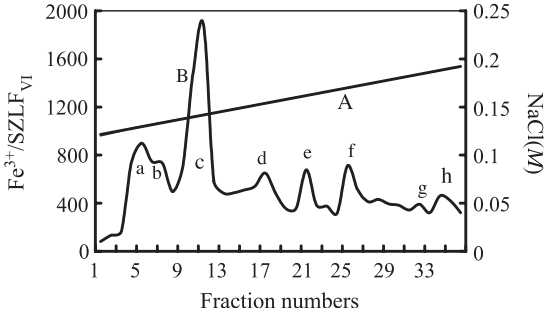

Fig. 1. Separation curve of the $SZLF_N$ samples containing varying iron numbers (left vertical coordinate) by ion-exchange chromatography equipped with DEAE-52 column under linear gradient elution of NaCl concentration ranging from 0.05 to 0.25 M. Curve A: linear curve of gradient elution of NaCl concentration ranging from 0.05 to 0.25 M (right vertical coordinate) for separating $SZLF_N$ samples. Curve B: absorbance curve of the ferritins having varying iron numbers within the their core as a function of fraction numbers. Forty-five percent of total protein of $SZLF_N$ shown in (c) sample was collected by gradient elution of 0.14 M NaCl, and its chemical compositions within the ferritin core are 1890 Fe^{3+}/$SZLF_{45\%}$ and 140 ± 10 P_i/$SZLF_{45\%}$. Fifty-five percent of total protein of $SZLF_N$ shown in (a), (b), (d), (e), (f), (g), and (h) samples was collected, and its chemical compositions within the ferritin core shows varying irons numbers ranging from 800 ± 50 Fe^{3+}/$SZLF_N$ to 420 ± 50 Fe^{3+}/$SZLF_N$.

About 45% of the $SZLF_N$ sample was collected by the gradient elution of 0.14 M NaCl at the absorbance peaks shown in Fig. 1c, called $SZLF_{45\%}$, having chemical composition consisting of 1890 ± 30 Fe^{3+}/$SZLF_{45\%}$ and 140 ± 10 P_i/ $SZLF_{45\%}$. In addition, a 13.5:1 ratio of iron to phosphate within the $SZLF_{45\%}$ core, called as HoloSZLF because it had the maximal iron numbers within the protein shell, was calculated according to its chemical composition. Another 55% of total $SZLF_N$ protein (Fig. 1a, b, d, e, f, g and h) was found to have $SZLF_{UI}$ characteristics, showing iron numbers ranging from 800 ± 50 Fe^{3+}/$SZLF_{UI}$ to 420 ± 50 Fe^{3+}/ $SZLF_{UI}$. The iron numbers within the $SZLF_{UI}$ core was clearly lower than that of $SZLF_{45\%}$, indicating that $SZLF_N$ is composed of holoSZLF (Fig. 1c) and $SZLF_{UI}$ in the liver cell of the shark before separated.

In order to understand the molecular size and electrophoresis mobility of both $SZLF_{45\%}$ and $SZLF_N$, both proteins are separated by PAGE at the same time. Interestingly, we found that both proteins showed similar mobility in the PAGE gel, indicating that the mixture of both ferritins was barely separated by normal PAGE. However, results in Fig. 1 showed clearly that the $SZLF_N$ samples consisting of $SZLF_{45\%}$ and $SZLF_{UI}$ could be separated by ion-exchange chromatography equipped with DEAE-52 column. It is well seen that the there are various negative charges on the surface of protein shell of the $SZLF_N$ samples due to the DEAE-cellulose, a separation gel with anion characteristics. Even so, like horse spleen ferritin (HSF), our experimental results further confirmed that both $SZLF_{45\%}$ and $SZLF_N$ had similar kinetic characteristics of complete iron release with biphasic behavior. It should be emphasized that this behavior is independent from the various iron numbers within the ferritin core. A factor of iron content within the ferritin core plays a minor role in formation of complex kinetics of iron release. However, according to the experimental results with abundant $SZLF_{UI}$ shown in Fig. 1, a novel process of iron storage in the liver cell of the shark or of other mammals in vivo is suggested as follows. First, the cell biosynthesized enough apoferritin for iron storage in vivo. Second, the apoferritin in part stored excess iron ions to form a holoferritin in the cell, and remnant apoferritin and ferritins with unsaturated iron always played a role in maintaining iron level as a nontoxic readily available form. We indicate that it is a reasonable novel mechanism for explaining for iron storage in vivo.

3.2. Molecular and subunit characteristics of $SZLF_E$ and $DALF_E$

In order to obtain the ferritin with high purity, $SZLF_{45\%}$ was further purified by PAGE, which is called $SZLF_E$. The $SZLF_E$ having identical iron numbers were used to study whether there is same molecular size of the core. The $SZLF_E$ was prepared by air drying small drops at copper grids for observing its molecular structure with electron microscopy. A transmission electron micrograph of $SZLF_E$ is shown in

Fig. 2. The molecular structure of $SZLF_E$ consists of a protein shell of 110–120 Å (11–12 nm) in over diameter and an iron core of 55–65 Å (5.5–6.5 nm) located at the center of the shell according to the bar size of the marker in Fig. 2. The molecular structure of $SZLF_E$ is consistent to that of native and reconstituted ferritins described previously [4,32]. In addition, examination of $SZLF_E$ (1890 Fe^{3+}/$SZLF_E$) revealed that the shape of the protein shell and the distribution of the core size were regular and identical in diameter (Fig. 2). Clearly, $SZLF_E$ is fit not only for the kinetic study of complete iron release by visible spectrometry at 520 nm but also for the mass measurement of the ferritin with MALDI-TOF MS because of the same iron numbers within the protein core.

Using the IEF technique, equine ferritin showed eight isoferritin bands with *p*I values ranging from 4.1 to 5.6 [26], and the DALF showed three isoferritin bands with *p*I values from 5.0 to 6.0 [30]. In order to understand charge distribution on the surface of $SZLF_E$, we would address another important question of whether the $SZLF_E$ molecules appear an identical *p*I values. However, our experimental results indicated that the holoDALF (2150 ± 50 Fe^{3+}/DALF) further purified by PAGE, called $DALF_E$, showed four isoferritin bands with different *p*I values ranging from 4.8 to 6.2 (Fig. 3, left lane), which the band numbers were somewhat higher than that reported recently by Kong et al. [30]. In addition, it is interesting to note that the $SZLF_E$ exhibited five isoferritin bands with different *p*I values ranging from 4.0 to 7.5 (Fig. 3, right lane). Clearly, the band numbers in $SZLF_E$ are more than that in $DALF_E$, although the iron numbers of ferritin core in the last are higher than that in the front. This phenomenon shows that the charge distribution on the surface of the $SZLF_E$ shell appears more complex than that of the DALF shell, which is independent on the iron numbers within the protein core, but it might depend on the composition of amino acids on the surface of the ferritin.

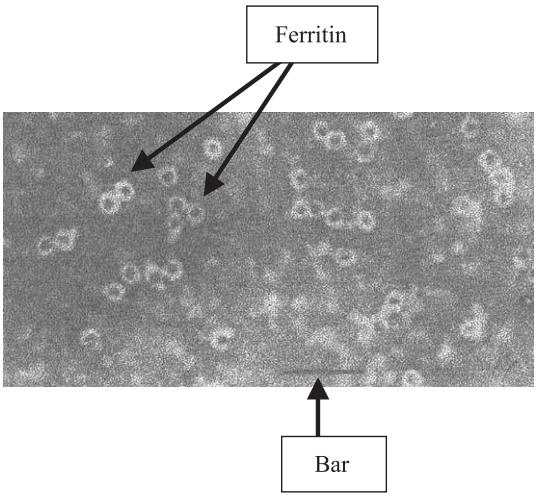

Fig. 2. Transmission electron micrographs of $SZLF_E$. Transmission electron micrographs (bar length: 50 nm) of negative staining from the $SZLF_E$. The sizes of the protein shell with 110–120 Å (11–12 nm) and the identical core size 55–65 Å (5.5–6.5 nm) within the ferritin core in diameter are observed according to the marker bar shown.

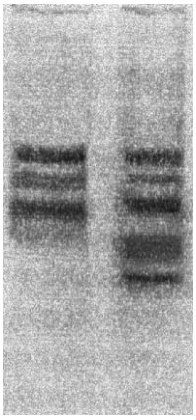

Fig. 3. $DALF_E$ (left lane) and $SZLF_E$ (right lane) electrophoretogram of isolelctric focusing. Left lane: $DALF_E$, four isoferritin bands with different *p*I values ranging from 5.0 to 6.0 in the gel; right lane: $SZLF_E$, five *iso*-ferritin bands with different *p*I values ranging from 4.0 to 7.0 in the IEF gel.

A recent report by Kong et al. [30] found that DALF was composed of H and L subunit types with molecular weights of 18 and 13 kDa, respectively, which showed a difference of 5 kDa for the subunits. In addition, HSF and DALF including other mammal ferritins are also composed of H and L subunit types with dispersion of 1–2 kDa [18,25,27,33–35]. Like horse and pig, the shark is also a vertebrate. However, Fig. 4 results show that $SZLF_E$ consists of single subunit type with the molecular weight of 21 ± 0.2

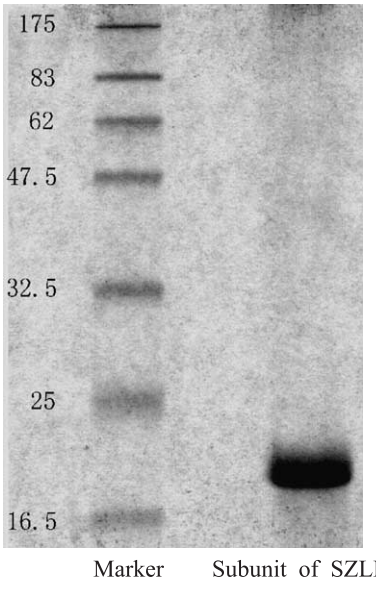

Fig. 4. Electrophorogram of the $SZLF_E$ subunit in the SDS-PAGE gel (Left lane: marker; right lane: the subunit of $SZLF_E$). The molecular weight of $SZLF_E$ subunit is calculated to be 21 kDa according to the markers of molecular weight of standard protein subunits and their mobility in the SDS-PAGE gel.

kDa in the SDS-gel according to the calculation of the reference markers, which is equal to the molecular weight of the H subunit from HSF. It is for this reason that another insight into the role of single subunit type from the SZLF for kinetic study of iron release should be studied further, which redounds to understand the real role of single subunit type from the SZLF in iron release and storage.

Tumor is one of main deadly diseases in mammal including human. Tumor is an outcome of cell growth in ruleless or in disorder in vivo. Moreover, the ferritin level in human serum increases greatly when human has caught a cancer, such as carcinoma, which means that a process of tumor formation needs an abundance of iron for synthesizing various proteins containing iron in vitro. In addition, bacteria in nature are organisms that have the cancer barely. Like bacterial ferritin with single type subunit, the shark ferritin might have capacities to control rate of iron release for restricting the growth of tumor cell in disorder in vivo, because its protein shell is consisted of single subunit type. That is why cancer was found hardly in the shark. It looks as if the association of these ideas is reasonable.

Molecular structure of most ferritins in nature is composed of 24 subunits. According to this conclusion and the molecular weight of the subunit shown in Fig. 4, molecular weight of $SZLF_E$ consisting of 24 subunits could be calculated to be 504 ± 2.4 kDa /$SZLF_E$, which is higher than that (440 kDa) of HSF as previously described. It is suggested that the electrophoresis mobility of $SZLF_E$ in PAGE gel should be lower than that of HSF. Contrarily, the experimental results that we did showed that the mobility of $SZLF_E$ in the PAGE gel exhibited somewhat quicker than that of HSF_E. One possibility we suggest is that both ferritins have quite different charges on the surface of both protein shells, which means that the charges of $SZLF_E$ are more than that of HSF_E. Another possibility is that the molecular size consisting of the single subunit type in diameter is less than that of HSF_E consisting of double subunit types. Both factors make that the mobility of $SZLF_E$ in PAGE-gel shows to be quicker than that of HSF_E at same electrophoresis time and reactive conditions even if the molecular weight in front was higher than that in later. The observation reported here suggests the charge distribution and amount on the surface of the ferritin shell play a more important role in carrying out its physiological function of iron release and storage than that of its molecular size. Thus, biological techniques of mass spectrometry such as ESI-TOF MS, MALDI-TOF MS, and MALDI-TOF/TOF MS might be used not only to study the variety and distribution of these charges on the surface of protein shell among ferritins, but also to investigate stability among the subunits coming from the different species. We suggest that the interaction intensity and the stability among the subunit from the ferritins be tightly connected with complex kinetics of iron release. However, the characteristics of mass spectrometry of the ferritins and its subunit are still unknown, because its molecular weight is too high to be measured by ESI-TOF MS or other techniques of MALDI-TOF MS directly.

3.3. Characteristics of mass spectra of SZLFE and its subunits

ESI- and MALDI-MS techniques provide a soft ionization for mass measurement of big biological molecules. The observation of coordinate-covalent and noncovalent binding complexes is now possible by using MALDI-MS. Mass analysis with MALDI-MS is typically performed with time-of-flight (TOF); resolving capabilities are on the orders ranging from 400 to 10 kDa, with accuracy ranging from 0.1% to 0.005%. MALDI can routinely analyze biological compounds from a mass of 0.5 to 200 kDa or greater and distinguish significantly different size of viral capsid protein, such as α and β protein [36]. It looks as if the laser coming from the MALDI–TOF mass spectrometer have the capacity to decompose the specific protein consisting of multisubunits with unstable characteristics into the free subunit. In order to understand whether there are same molecular masses in the $SZLF_E$ sample because of same iron numbers in the ferritin, a technology of MALDI-TOF MS is selected to measure the ferritin mass and analyze the stability among its subunits.

Using MALDI-TOF MS, we found that the laser coming from the MALDI-TOF mass spectrometer could not make $SZLF_E$ to form a whole protein ion for its mass measurement in the presence of SA or of other matrix, because its molecular weight of 504 ± 2.4 kDa is too big to form a molecular ion. With the same condition, similar results from the HSF, PSF, and DALF are observed directly. Interestingly, four ion peaks of $SZLF_E$ subunits at *m*/*z* 10611.07, 21066.52, 41993.16, and 63555.64 were clearly observed under the condition of high laser intensity (Fig. 5). However, this behavior was not found by the low laser intensity. The ion peaks at *m*/*z* 21066.52 close to molecular weight (21 kDa) of $SZLF_E$ subunit determined by SDS-PAGE (Fig. 4) is called as subunit mass of $SZLF_E$ with single charge $[M]^+$. In addition, *m*/*z* among four mass peaks shown in Fig. 5 appears a multiple relation according to their charges and masses. Evidently, four peaks at *m*/*z* 10611.07, 21066.52, 41993.16, and 63555.64 were identified as $[M]^{2+}$, $[M]^+$, $[2M]^+$, and $[3M]^+$, respectively. Although the high laser intensity does not have the capacity to make the $SZLF_E$ form molecular ions in the presence of matrix SA, it can weaken binding energy of noncovalent bonds among subunits of $SZLF_E$ and decompose the ferritin into the subunit and its polymers for mass measurement in the presence of SA (Fig. 5).

A proposed process for ion formation and mass measurement of ferritin subunit and its polymers was shown in Fig. 6, in which major characteristics are summarized as follows: (1) it is interesting to note that the peaks of mass spectra from the $SZLF_E$ subunit were observed unlikely (Fig. 6E), while the low laser intensity (Fig. 6C) is used in

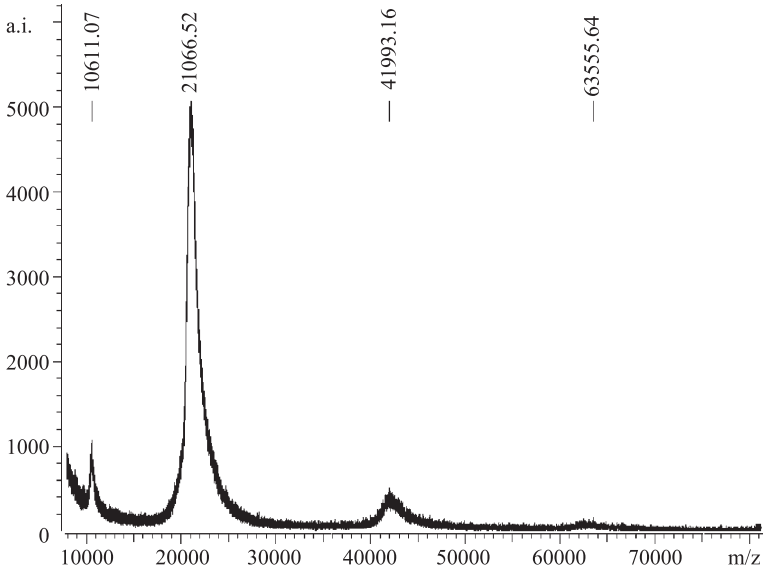

Fig. 5. Mass spectra of $SZLF_E$ subunits and its polymers with measurement of MALDI-TOF MS. The *m/z* at the peaks shown gives the molecular mass of $SZLF_E$ subunits and its polymers. A dominant peak at *m/z* 21066.52 corresponds to $SZLF_E$ subunit with single charge (M^+). Second dominant peak at *m/z* 10611.07 corresponds to the subunit with double charges (M^{2+}). Other peaks at *m/z* 41993.16 and 63555.64 are considered to show the subunits having single charge with dimmer ($2M^+$) and trimmer ($3M^+$) structure, respectively.

the presence of matrix SA. (2) The subunit mass peaks of $SZLF_E$ (Fig. 6G) are directly observed by the treatment with the high laser intensity (Fig. 6F) in the presence of matrix SA. (3) The matrix SA plays a minor role in forming molecular iron of $SZLF_E$ subunit for mass measurement without the aid of the high laser intensity. Moreover, these novel phenomena shown in Figs. 5 and 6 indicate that there are weakened interaction among the subunits with single type in the $SZLF_E$, in which results into the unstable subunit being directly transferred into the molecular ion for mass measurement by the high laser intensity in the presence of SA. Thus, we suggest that this interaction (regulation) among the subunits of $SZLF_E$ might participate in the iron release and storage even if the ferritin consists of 24 subunits with single type. In order to confirm this suggestion, further kinetic study of complete iron release from the in vivo and in vitro should be considered.

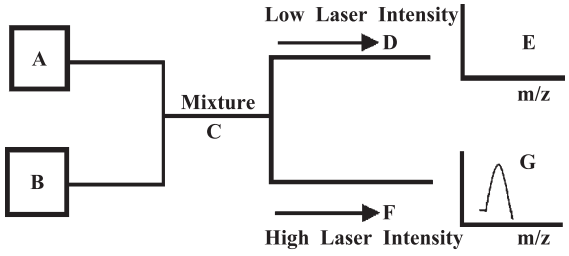

Fig. 6. A proposed process of mass measurement of ferritin subunit under the different laser intensity in the absence of matrix SA. (A) Matrix SA; (B) $SZLF_E$ sample; (C) mixture of SA and $SZLF_E$; (D) low laser intensity; (E) mass spectrogram of $SZLF_E$ subunit under the condition with low laser intensity; (F) high laser intensity; (G) mass spectrogram of $SZLF_E$ subunit under the condition with high laser intensity.

3.4. Kinetics of iron release from the $SZLF_E$

We next address another question of whether $SZLF_E$, which is consisted of single subunit type, is able to show simple kinetics for complete iron release with single-phase behavior, because HSF and PSF consisting of H and L subunits show complex kinetics with biphasic behavior. Results in Fig. 7 show a kinetic process of complete iron release from the $SZLF_E$ in vitro. Kinetic curve shown in Fig. 7 does not follow laws of either zero-, first-, or second-order reactions, indicating that $SZLF_E$ still appears, like HSF, the complex kinetics of iron release with biphasic behavior even

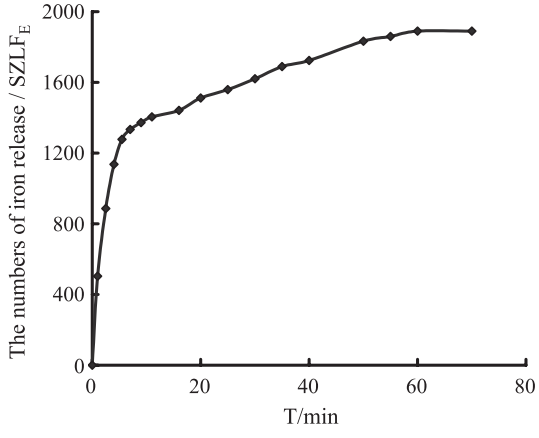

Fig. 7. Kinetics of complete iron release from the $SZLF_E$ at pH 7.25. A plot of the numbers of iron release per molecular $SZLF_E$ monitored at 520 nm as a function of time gives complex kinetics process with biphasic behavior. The reaction time for complete iron release is estimated to be about 60 min, in which the maximal numbers of iron release from the $SZLF_E$ is 1890 $Fe^{3+}/SZLF_E$.

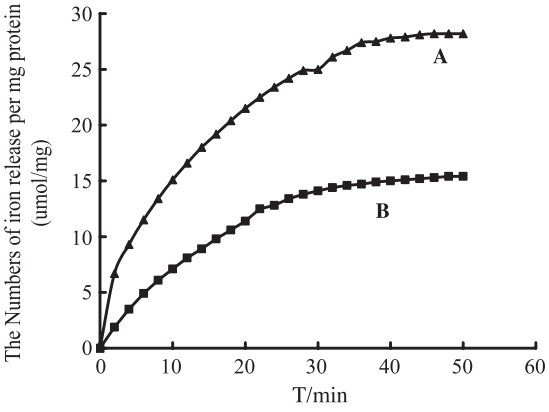

Fig. 8. Kinetics of complete iron release from the liver extraction of *S. zygaena*. Kinetics of complete iron release from the crude extraction from the liver of *S. zygaena* was measured by a spectrophotometry at 520 nm after the extraction was treated at temperatures of 30 and 60 °C, respectively. A plot of the numbers of iron release per milligram of protein monitored at 520 nm as a function of time gives a complex kinetic process at each curve. Two curves shown in Fig. 5 did not follow either zero-, first-, or second-order reactions. Treating temperature: 60 °C (curve A) and 30 °C (curve B).

if it consists of single subunit type. The results in Figs. 1–6 have demonstrated that the charge difference on the surface of ferritin shells, the types of single subunit, and the identical iron numbers within the $SZLF_E$ core cannot make the complex kinetics of complete iron release with biphasic behavior transfer into a simple that is with single-phase behavior. Despite the biphasic behavior of iron release that can be found in vitro, we still doubt whether there is another kinetic pathway for iron release from the ferritin with single-phase behavior in vivo, because it can interact with other proteins and big biological molecules in the cell. It is suggested that these big molecules in vivo can directly regulate and limit the ferritin to release iron from simple kinetics. The observation reported here indicates that crude extraction of the shark liver is an ideal model with interactions of both ferritin and other proteins for studying kinetics of complete iron release.

In order to understand whether other proteins in the liver cell of the shark participate in the reaction of iron release of the SZLF, the crude extraction of the shark liver is used to study the process of iron release under the condition of different reactive temperature. Fig. 8 results show two kinetic curves of complete iron release from the crude extraction at treatment temperature of 30 and 60 °C for 60 min, respectively. According to the two kinetic curves shown in Fig. 8, the plot of numbers of iron release per milligram of protein of the extraction monitored as 520 nm as a function of time does not fit for laws of a zero-, first-, or second-order reaction, which is similar to that of $SZLF_E$ (Fig. 7) in vitro. In addition, rate of iron release in Fig. 8A is higher than that of Fig. 8B, because the ferritin concentration per milligram of protein in front is higher than that in later. The observation reported here concludes that the proteins in the crude extraction participate in the iron release and play a minor role in forming complex kinetics of iron release with biphasic behavior from the ferritin. It is indicated that SZLF in vitro and in vivo shows similar kinetic behaviors of iron release. The regulation capacity of the SZLF shell with interaction among the subunits is considered to play an important role in forming the complex kinetics of iron release with biphasic behavior, which is independent of the ferritin subunit types. It is for this reason that HSF consisting of double subunit types and SZLF consisting of single subunit type show similar kinetic characteristics of complete iron release.

3.5. Released ratio of phosphate to iron within the $SZLF_E$ core

Our previous study with HSF demonstrated that two released ratios of phosphate to iron with the ferritin core are clearly divided, which describes an iron structure with 1:3 ratio on the surface of the HSF core, another one with 1:13 ratio on the inside of it [9,14]. This phenomenon shows that the ratio across the ferritin core appears barely identical. The experiments using $SZLF_E$ with released ratio of P_i to Fe^{3+} across the protein core (Fig. 9) demonstrate that a plot of released P_i concentration as function of released Fe^{3+} numbers within the protein core resembles a linear relation with an identical released ratio (1:13.2) of P_i to Fe^{3+}, which differs from that of HSF with biphasic behavior described previously [14]. Unlike mammal ferritin, $SZLF_E$ has a novel structure of iron core with the identical ratio. Even so, $SZLF_E$ still shows complex kinetics of iron release with biphasic behavior (Figs. 7 and 8). Clearly, this identical ratio is an unimportant factor of forming complex kinetics, because $SZLF_E$ and other mammal ferritins show similar kinetic characteristics, but just what of this structure of iron core in the $SZLF_E$ remains is still a question in understand-

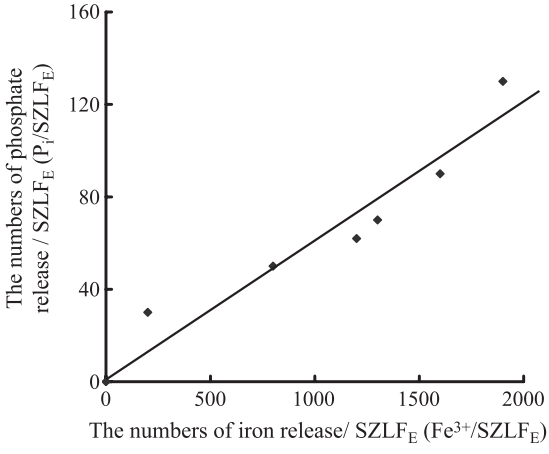

Fig. 9. Measurement of released ratio of phosphate to iron within the $SZLF_E$ core along with iron release increment. A plot of released P_i concentration as function of released iron numbers within the $SZLF_E$ core gives a linear relation. An identical released ratio (1:13.2) of phosphate to iron within the $SZLF_E$ core was observed by a process of complete iron release at pH 7.25.

ing the ferritin behavior and showing no cancer diseases in the shark.

3.6. Conclusion

According to the experimental results shown in Figs. 1–9, we found that several factors played a minor role in forming complex kinetics of complete iron release with biphasic behavior. These factors are summarized to be the charge difference on the surface of the ferritin shell, the subunits types, the identical or varying ratio of P_i to Fe^{3+} within the ferritin core, and the interaction of both ferritin and other proteins. Results of MALDI-TOF MS have indicated that the ferritin shows the characteristics of weaken interaction among its subunits (Fig. 5). It is for this reason that we indicate that the regulation capacities of protein shell itself [9] by interaction among the subunits play a limited step for controlling a different rate of iron release and an important role in forming complex kinetics of complete iron release with biphasic behavior. However, with reference to previous research, very little information about the role of the interaction among subunits of various ferritins has importance been attached to explain the mechanism of iron release and storage including other functions, such as trapping various heavy metal ions [37] in vitro or in vivo.

Acknowledgements

This work was supported by the Natural Science Fund of China (No. 40276033), the Foundation of Fujian Provincial Natural Science in China (No. C0310006), the Graduate Scholarship Program of Xiamen University, and by the Foundation of Xiamen Natural Science in China (No.3502Z2001262).

References

[1] H.Q. Huang, R.K. Watt, R.B. Frankel, G.D. Watt, Role of phosphate in Fe^{2+} binding to horse spleen holoferritin, Biochemistry 32 (1993) 1681–1687.
[2] F. Goto, Y. Toshiro, S. Naoki, et al., Iron fortification of rice seed by the soybean ferritin gene, Nat. Biotechnol. 17 (1999) 282–286.
[3] E.C. Theil, H. Takagi, G.W. Small, et al., The ferritin iron entry and exit problem, Inorg. Chim. 297 (2000) 242–251.
[4] J. Lee, S.W. Kim, Y.H. Kim, J.Y. Ahn, Active human ferritin H/L-hybrid and sequence effect on folding efficience in *Escherichia coli*, Biochem. Biophys. Res. Commun. 298 (2002) 225–229.
[5] G.D. Watt, J.W. McDonald, C.H. Chiu, K.R.N. Reddy, Further characterization of the redox and spectroscopic properties of *Azotobacter vinelandii* ferritin, J. Inorg. Biochem. 51 (1993) 745–758.
[6] P.M. Harrison, T.G. Hoy, I.G. Macara, et al., Ferritin iron uptake and release, Biochem. J. 143 (1974) 445–451.
[7] S. Mann, J.M. Williams, A. Treffry, P.M. Harrison, Reconstituted and native iron-cores of bacterioferritin and ferritin, J. Mol. Biol. 198 (1987) 405–416.
[8] F. Funk, J.P. Lenders, R.R. Crichton, et al., Reductive mobilisation of ferritin iron, Eur. J. Biochem. 152 (1985) 167–172.
[9] H.Q. Huang, Q.M. Lin, B. Kong, et al., Role of phosphate and kinetic characteristics of complete iron release from native pig spleen ferritin-Fe, J. Protein Chem. 18 (1999) 497–504.
[10] T.G. Hoy, P.M. Harrison, M. Shabbir, et al., The release of iron from horse spleen ferritin to 1,10-phenanthroline, Biochem. J. 137 (1974) 67–70.
[11] H.Q. Huang, F.Z. Zhang, C.H. Chen, et al., Studies on kinetics of iron release from bacterial ferritin of *Azotobacter vinelandii*, Acta Biophys. Sin. 12 (1996) 33–38.
[12] T. Jones, R. Spencer, C. Walsh, Mechanism and kinetics of iron release from ferritin by dihydroflavins and dihydroflavin analogues, Biochemistry 17 (1978) 4011–4017.
[13] T.M. Richards, K.R. Pitts, G.D. Watt, A kinetics study of iron release from *Azotobacter vinelandii* bacterial ferritin, J. Inorg. Biochem. 61 (1996) 1–13.
[14] H.Q. Huang, R.K. Watt, G.D. Watt, et al., The properties of the surface of iron core from horse spleen ferritin, J. Xiamen Univ. (Natural Science, Chinese) 32 (1993) 628–663.
[15] H.Q. Huang, Q.M. Lin, T.L. Wang, Kinetics of iron release from pig spleen ferritin with bare platinum electrode reduction, Biophys. Chemist. 97 (2002) 17–27.
[16] J.L. Johnson, M. Cannon, R.K. Watt, et al., Forming the phosphate layer in reconstituted horse spleen ferritin and role of phosphate in promoting core surface reactions, Biochemistry 38 (1999) 6706–6713.
[17] D.M. Lawson, P.J. Artymiuk, S.J. Yewdall, et al., Solving the structure of human H ferritin by genetically engineering intermolecular crystal contacts, Nature 349 (1991) 541–544.
[18] J.K. Grady, J. Zang, T.M. Laue, P. Ariso, et al., Characterization of the H- and L-subunit ratios of ferritins by sodium dodecyl sulfate-capillary gel electrophoresis, Anal. Biochem. 302 (2002) 263–268.
[19] M.C. Linder, G.M. Nagel, M. Roboz, et al., The size and shape of heart and muscle ferritin analyzed by sedimentation, gel filtration, and electrophoresis, J. Biol. Chem. 256 (1981) 9104–9110.
[20] J.R. Mertz, E.C. Theil, Subunit dimers in sheep spleen apoferritin, J. Biol. Chem. 258 (1983) 11719–11726.
[21] K.S. Park, H. Kim, N.Y. Kim, et al., Proteomic analysis and molecular characterization of tissue ferritin light chain in hepatocellular carcinoma, Hepaol 35 (2002) 1460–1466.
[22] E.R. Rocha, S.C. Andrews, J.N. Keen, J.H. Brock, Isolation of a ferritin from *Bacteroides fragilis*, FEMS Microbiol. Lett. 95 (1992) 207–212.
[23] K.S. Kim, H.R. Mun, J.H. Lee, Iron cores of tadpole ferritin: native, reconsistuted and recombinant H-chain ferritins, Inorg. Chim. Acta 298 (2000) 107–111.
[24] K. Watanade, K. Hazuhiro, T. Miyamoto, et al., Characterization of ferritin and ferritin-binding protein in cannine serum, BioMetals 13 (2000) 57–63.
[25] S.N. Wai, T. Takata, A.T.N. Hamasaki, K. Amako, Purification and characterization of ferritin from *Campylobacter jejuni*, Arch. Microbiol. 164 (1995) 1–6.
[26] C. Geetha, V. Deshpande, Purification and characterization of liver ferritins from different animal species, Comp. Biochem. Physiol. B 123 (1999) 194–285.
[27] S. Levi, J. Safrld, F. Franceschinelli, A. Cozzi, et al., Expression and structural and functional of human ferritin L-chain from *Escherichia coli*, Biochemistry 28 (1989) 5179–5184.
[28] I. Olcay, A. Kars, F. Kocabeyoglu, Serum levels of Ca125, ferritin and tissue polypeptide antigen in lung cancer and benign diseases of the lung, Lung Cancer 18 (1997) 223.
[29] M.K. Ali, A. Akhmedkhanov, A. Zeleniuch-Jaquotte, et al., Reliability of serum iron, ferritin, nitrite, and association with risk of renal cancer in women, Cancer Detec. Prev. 27 (2003) 116–121.
[30] B. Kong, H.Q. Huang, Q.M. Lin, et al., Purification, electrophoretic behavior, and kinetics of iron release of liver ferritin of *Dasyatis akajei*, J. Protein Chem. 22 (2003) 61–70.
[31] T. Cooper, Tools of Biochemistry, Wiley, New York, 1997, p. 53.

[32] V.J. Wade, S. Levi, P. Arosio, et al., Influence of site-directed modifications on the formation of iron cores in ferritin, J. Mol. Biol. 221 (1991) 1443–1452.
[33] M.J. Hudson, S.C. Adrews, C. Hawkins, et al., Overproduction, purification and characterization from the *Escherichia coli* ferritin, J. Biochem. 218 (1993) 985–995.
[34] K. Orino, K. Eguchi, T. Nakayama, et al., Sequencing of cDNA clones that encode bovine ferritin H and L chains, Comp. Biochem. Physiol. 118B (1997) 667–673.
[35] G. Sobha, S. Suryakala, C. Geetha, V. Deshpande, Camel kidney ferritin: isolation and partial characterization, Vet. Res. Commun. 24 (2000) 287–297.
[36] S.A. Trauger, W. Webb, S. Gary, Peptide and protein analysis with mass spectrometry, Spectroscopy 16 (2002) 15–28.
[37] H.Q. Huang, T.M. Cao, Q.M. Lin, Characteristics of trapping copper ions with scrolled ferritin reactor in the flowing seawater, Environ. Sci. Technol. 38 (2004) 2476–2481.